Tribology International 209 (2025) 110728

Contents lists available at ScienceDirect

Tribology International

journal homepage: www.elsevier.com/locate/triboint

Prediction of fretting fatigue lifetime of dovetail joints using a Modified Theory of Critical Distances

Qiqi Xiao [a], Can Wang [a], Bilal Ahmed [a], Dagang Wang [b], Zhenbing Cai [c], Lihua Wang [d,*], Magd Abdel Wahab [a,e,f,**]

[a] Soete Laboratory, Department of Electrical energy, metals, mechanical constructions and systems, Faculty of Engineering and Architecture, Ghent University, Belgium
[b] School of Mechatronic Engineering, China University of Mining and Technology, Xuzhou 221116, China
[c] Tribology Research Institute, Southwest Jiaotong University, Chengdu 610031, China
[d] School of Aerospace Engineering and Applied Mechanics, Tongji University, Shanghai 200092, China
[e] College of Engineering, Yuan Ze University, Taiwan, China
[f] Parallel and Distributed Systems Laboratory, Jožef Stefan Institute, Jamova cesta 39, Ljubljana SI-1000, Slovenia

ARTICLE INFO

Keywords:
Dovetail joints
Stress gradient
Principal stress
Critical distance
Crack angle
Initiation lifetime

ABSTRACT

Dovetail joints are widely used in mechanical systems and aerospace applications. Under cyclic loading conditions, they are susceptible to fretting fatigue, which can lead to premature failure. Therefore, improving the accuracy of lifetime prediction under fretting fatigue is crucial. In dovetail joints, fretting conditions result in a complex stress-strain distribution on the contact surface, affecting the applicability of different failure criteria. This study examines the stress states across various models and evaluates the suitability of each criterion accordingly. The accuracy of crack initiation angle prediction for two types of dovetail joints is improved. The maximum principal stress serves as a reference for extreme stress, while the stress gradient describes the rate of change in stress. The combination of stress gradient and maximum principal stress provides a more comprehensive representation of stress distribution. The traditional Theory of Critical Distances (TCD) is unable to effectively address the complex stress distribution in stress concentration areas. To overcome this limitation, a Modified TCD (MTCD) is proposed, integrating the effects of stress gradients and maximum principal stress into the original TCD framework. The MTCD method significantly improves the accuracy of predicting the initiation lifetime of both dovetail joints compared to the traditional TCD method. This study not only enhances the understanding of fretting fatigue behavior in dovetail joints but also provides a reliable predictive tool for evaluating more complex models of dovetail joints.

1. Introduction

The phenomenon when materials experience fatigue fracture due to friction caused by slight relative movement between two contacting surfaces under cyclic loading is called fretting fatigue [1–3]. It frequently occurs in mechanical joints, bearings, gears, and bolted connections. This paper concentrates on the study of fretting fatigue in dovetail joints of aircraft blades. Under the action of fretting, the local areas of the contact surface experience slight relative slippage due to vibrations. The friction between the rough surfaces causes localized material detachment, generating wear particles. These wear particles exacerbate the damage to the contact surface and lead to stress concentration on the material surface [4,5]. Small cracks initiate in the stress concentration areas and gradually propagate from the contact surface into the material, eventually leading to fatigue fracture of the material.

Fretting fatigue lifetime is defined as the number of cycles from the onset of loading to the point of final fracture. Crack initiation and crack propagation are two categories, into which fretting fatigue lifetime is generally divided. The research conducted by Poovakaud et al. [6] found that the initiation phase consumed the vast majority of fatigue lifetime, accounting for approximately 85 %. Sadeghi et al. [7] founded that

* Corresponding author.
** Corresponding author at: Soete Laboratory, Department of Electrical energy, metals, mechanical constructions and systems, Faculty of Engineering and Architecture, Ghent University, Belgium.
E-mail addresses: lhwang@tongji.edu.cn (L. Wang), magd.abdelwahab@ugent.be (M. Abdel Wahab).

https://doi.org/10.1016/j.triboint.2025.110728
Received 9 November 2024; Received in revised form 9 April 2025; Accepted 13 April 2025
Available online 14 April 2025
0301-679X/

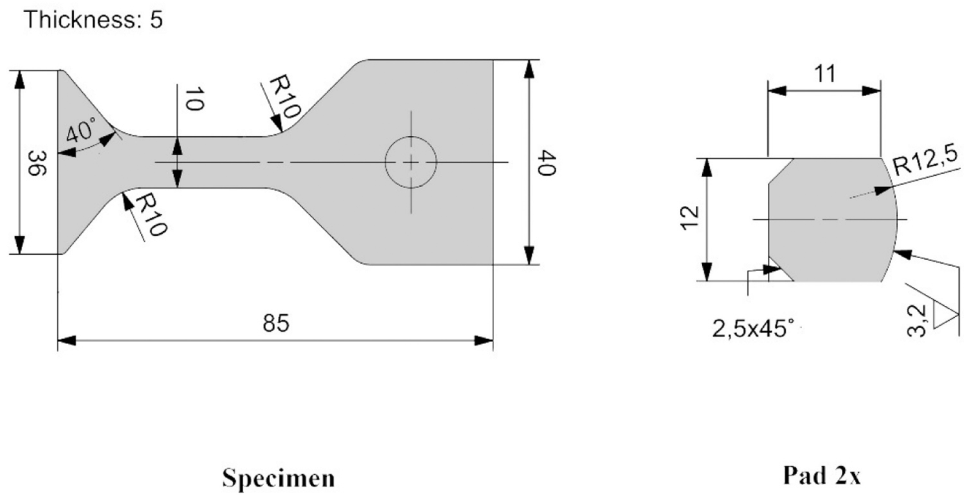

Fig. 1. The geometric dimensions for the dovetail joint with pads [9].

under high-cycle fatigue conditions, the crack initiation lifetime constituted the majority of the total fatigue lifetime, reaching up to 90 % in some cases. Szolwinski and Farris [8] conducted several fretting fatigue tests, the results showed that the initiation lifetime accounted for approximately 85–90 % of the total fatigue lifetime. The investigation by Sunde et al. [9] indicated that the initiation lifetime is the critical stage of fretting fatigue lifetime, accounting for 85–95 % of the total lifetime for dovetail joints. Therefore, crack initiation lifetime accounts for a significant portion of the total fatigue lifetime and predicting it is crucial. Accurately predicting crack initiation lifetime and understanding the mechanisms behind crack initiation enable the proactive implementation of preventive measures. This can be achieved through material selection and design optimization, ultimately improving the overall lifetime of the structure.

The Critical Plane (CP) theory is an important and efficient theory for predicting the fretting fatigue behaviour of materials. CP theory is applied to materials under multiaxial stress states, suggesting that crack initiation and propagation occur on a critical plane within the material [10,11]. Based on this theory, damage parameters such as Findley Parameter (FP), Fatemi-Socie (FS) and Smith-Watson-Topper (SWT), are used to evaluate fatigue lifetime. Among them, the SWT parameter takes into account the effects of both stress and strain in a comprehensive manner, and it performs well in the lifetime predictions of both Low-Cycle Fatigue (LCF) and High-Cycle Fatigue (HCF) [12].

However, during the implementation of these theories, it was found that the stress concentration phenomenon at the contact surfaces led to a significant stress gradient within the contact area. If the maximum value is used to predict fatigue lifetime, the results are often overly conservative. Therefore, researchers proposed the TCD method to mitigate the impact of stress concentration on the prediction results [13].

Zhu and Chen [14] found that the variable-TCD combined with the Mesh Control method (TCD-MC) provided a more reasonable and accurate approach for establishing the critical distance, based on their analysis of fretting fatigue tests conducted on two different dovetail joint models. Araújo et al. [15] developed a new lifetime prediction method by combining TCD and Modified Wöhler Curve Method (MWCM) to account for the multiaxiality of the stress in the fatigue failure region. This method improved the accuracy of fatigue lifetime prediction. Shi et al. [16] significantly improved the accuracy of fatigue lifetime prediction by modifying the traditional SWT model through the introduction of an average SWT parameter at a specific distance between the contact surface and the material's interior. Shen et al. [17] studied the influence of stress gradient on the critical distance by conducting fatigue tests on notched specimens with varying geometries. Based on their findings, they introduced the stress gradient method, concluding that

Table 1
The fretting fatigue test results for the dovetail joint with pads [9].

Test No.	Applied Stress (MPa)	N_f (cycles)
WP-T1	60	> 2e6
WP-T2	70	> 2e6
WP-T3	75	1016966
WP-T4	80	1025609
WP-T5	80	1869836
WP-T6	84	1293027
WP-T7	85	1648296
WP-T8	90	952207
WP-T9	96	722932
WP-T10	100	379972
WP-T11	100	624729
WP-T12	104	724374
WP-T13	110	590233
WP-T14	120	313831
WP-T15	130	284403

this method offered more accurate lifetime predictions under HCF conditions. Zhu and Chen [18] proposed the Gradient-TCD method, using the stress difference between adjacent points from the maximum stress on the contact surface to a specified distance within the material as a reference. The results showed that the Gradient-TCD exhibited better and more consistent performance.

Many scholars have conducted extensive research on the optimization of TCD theory, but its application to dovetail joints remains relatively limited. Meanwhile, combining the stress gradient and the maximum principal stress is essential to describe the complex stress distribution in the stress concentration area. Both factors play a crucial role in the determination of the critical distance. Thus, this paper presents the influence of maximum principal stress and stress gradient on the determination of the critical distance for the first time. This further improves the accuracy of fatigue lifetime prediction.

2. Experiments

2.1. Dovetail joint with pads model

This is a new type of fretting fatigue testing device based on dovetail joint, developed by Sunde et al. [9]. The contact configuration is cylinder-to-flat style. The device allows for easy replacement of contact pads, enabling tests with different contact geometries and surface treatments by simply switching the pads. It is currently a widely used device for dovetail joint fretting fatigue testing. The geometric dimensions involved in the test are shown in Fig. 1.

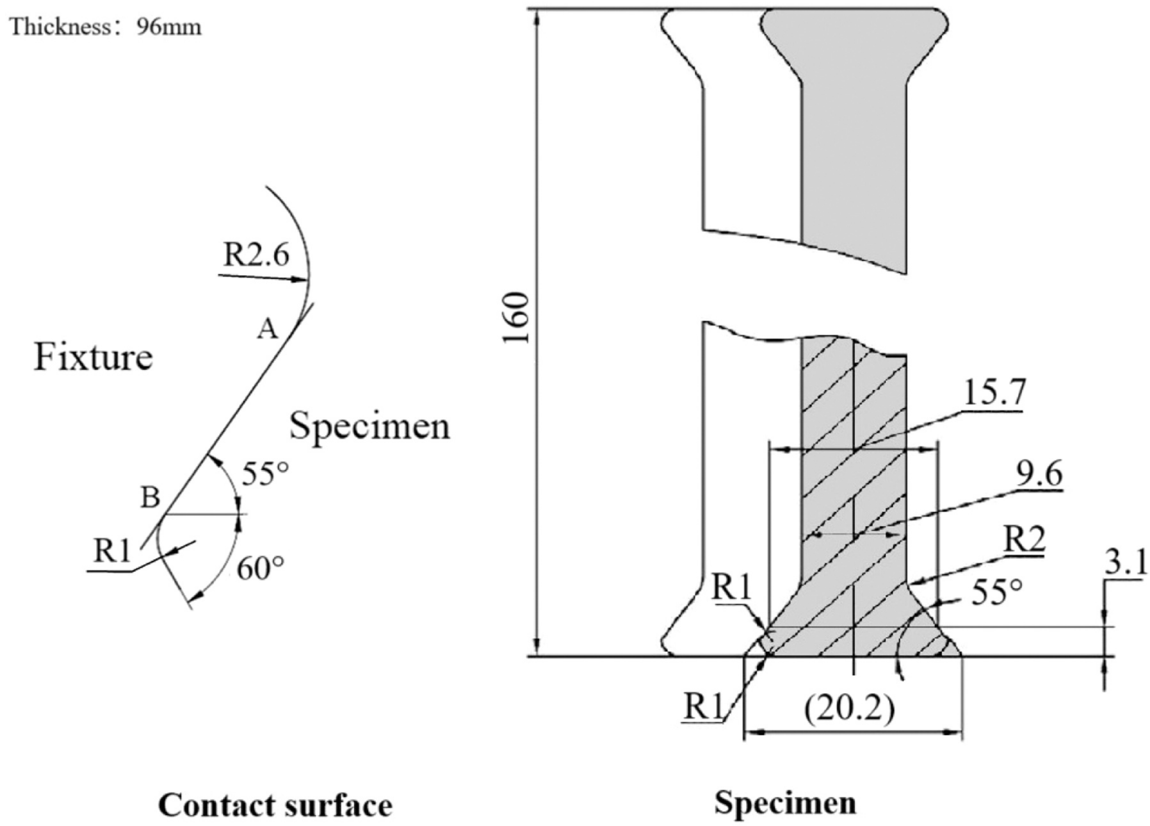

Fig. 2. The geometric dimensions for the traditional dovetail joint [19].

Table 2
The fretting fatigue test results for the dovetail joint with pads [19].

Test No.	Applied Stress (MPa)	N_f (cycles)
T-T1	175	74700
T-T2	208	62408
T-T3	228	39025

Both the specimen and the fretting pads are made of Ti6Al4V material with a Young's modulus of 115 GPa and a Poisson's ratio of 0.32. Fifteen fretting fatigue tests were conducted [9] by using this device, and the results of these tests are listed in Table 1. The test numbers for the dovetail joint are prefixed with pads.

2.2. Traditional dovetail joint model

Hu et al. [19] designed and tested a sub-scale specimen and fixture for dovetail joints in fretting fatigue tests under cyclic loading. In this

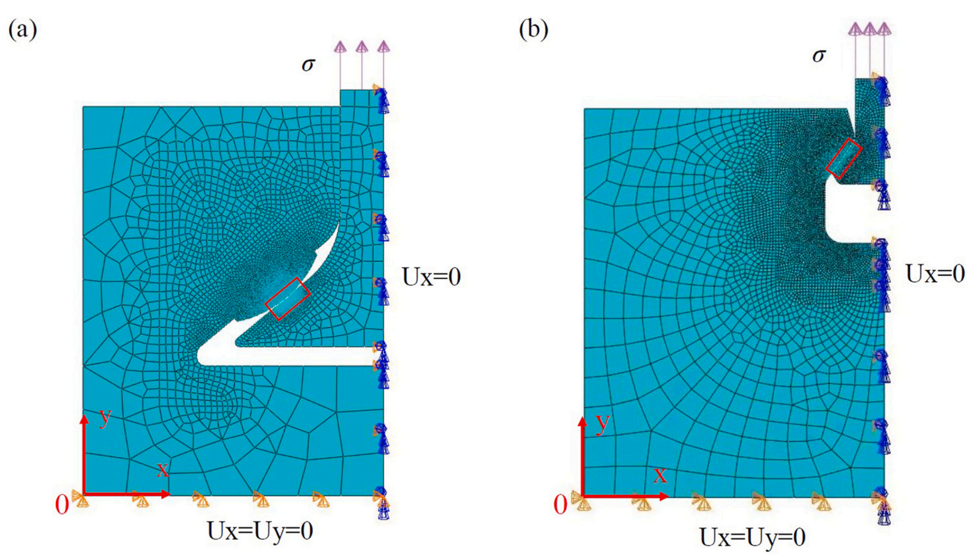

Fig. 3. The finite element models: (a) dovetail joint with pads and (b) traditional dovetail joint.

test, the contact area utilized a flat-to-flat contact configuration. The geometric dimensions involved in the test are shown in Fig. 2.

For the traditional dovetail joint model, Ti6Al4V is also used as the experimental material. However, there are slight differences in the material properties between the two. The experimental material in this model has an elastic modulus of 109 GPa and a Poisson's ratio of 0.34. Three fretting fatigue tests were conducted using this model, and the results of these tests are listed in Table 2. The test numbers for the traditional dovetail joint are prefixed with 'T'.

3. Numerical models

Both 3D and 2D models are commonly used to study the fretting fatigue behaviour of dovetail joints. 3D models can fully capture the geometry and loading conditions, providing a more detailed representation of the structure. However, previous research [20] has shown that the stress distribution along the thickness direction in 3D models remains nearly unchanged. This suggests that 2D modelling is sufficient for accurately analysing such structures without significant loss of precision. Based on these findings, this study adopts a 2D modelling approach, which ensures both accuracy and computational efficiency for fretting fatigue analysis. 2D plane strain finite element models were created in ABAQUS, as shown in Fig. 3. As one specimen has a thickness of 5 mm and a neck width of approximately 10 mm, as shown in Fig. 1, and the other specimen has a thickness of 96 mm and a neck width is 9.6 mm as shown in Fig. 2, a plane strain assumption is considered appropriate for both cases. A linear elastic constitutive relationship is used for the simulation. The element type is CPE4, a 4-node plane quadrilateral element. Considering that the entire structure is symmetric, only half of the model is taken for simulation calculations, and symmetric boundary conditions are applied along the symmetric axis. The bottom surface of the fixture is fixed in both the x and y directions. For the dovetail joint with pads model, a uniformly distributed load with a stress ratio of 0.1 is applied to the top of the specimen, as shown in Fig. 3(a). For the traditional dovetail joint model, a uniformly distributed load with a stress ratio of 1/16 is applied to the top of the specimen, as shown in Fig. 3(b). Due to the significant stress variation and steep stress gradient in the contact area, finer meshing is required to obtain more accurate stress-strain information. In this study, the element size in the contact area is refined to 2 μm. To balance computational efficiency, mesh refinement is applied only to a localized region near the contact area, as highlighted by the red box in Fig. 3.

In ABAQUS, two algorithms are typically provided to solve contact problems: the penalty method and the Lagrange multiplier method. In this study, we chose the surface-to-surface contact approach instead of node-to-node contact. This decision is made because the surface-to-surface method provides a more accurate and stable solution by distributing contact constraints over an entire surface rather than concentrating them at discrete nodes, which helps to avoid excessive stress localization and numerical instability. The Lagrange multiplier method is more accurate as the normal load remains constant for standard fretting fatigue simulations. In the fretting fatigue simulation of dovetail joints, convergence difficulties and noticeable instability can arise. The penalty method, which allows for slight penetration, provides better convergence and adaptability when addressing contact issues in the dovetail joint model. Zhu and Chen's [14] research also indicates that the results obtained from the two contact algorithms show minimal differences. Therefore, the penalty method is used to handle the contact problems in this paper. For the dovetail joint with pads model, a coefficient of friction of 0.55 is used, whereas for traditional dovetail joint model, the coefficient of friction is set to 0.5.

Table 3
The fatigue parameters of the different materials applied to the two dovetail joints [16,19].

Model type	σ_f'(MPa)	ε_f'	b	c
Dovetail joint with pads	2030	0.841	−0.104	−0.688
Traditional dovetail joint	1460.16	0.33777	−0.10124	−0.60152

4. Methodology

4.1. Critical plane theory

As mentioned in the introduction section, three CP parameters are used, namely FP, FS, and SWT. Among them, Findley proposed a damage parameter applicable to HCF, known as the FP parameter [21]. Its mathematical expression is shown in Eq. (1):

$$FP = \frac{\Delta\tau_{\max}}{2} + k_1\sigma_n^{\max} = \tau_f'(2N_i)^{b'} \tag{1}$$

where $\Delta\tau_{\max}$ and $\sigma_n^{\max}$ are the maximum shear stress amplitude and the maximum normal stress on the critical plane, k_1 is a material-dependent correction factor related to sensitivity of normal stress to fatigue lifetime that can be easily determined through fatigue tests. FP is used to derive the crack initiation lifetime. τ_f' is the shear fatigue strength coefficient, N_i is initiation lifetime and b' is the fatigue strength exponent in torsion. Analysing Eq. (1), the FP parameter primarily focuses on the amplitude of the maximum shear stress, with the introduction of the maximum normal stress for correction to better predict crack initiation.

Fatemi and Socie proposed the FS parameter based on multiaxial fatigue tests under in-phase and out-of-phase loadings [22]. This damage parameter is suitable for LCF and its mathematical expression is shown in Eq. (2):

$$FS = \frac{\Delta\gamma_{\max}}{2}\left(1 + k_2\frac{\sigma_n^{\max}}{\sigma_y}\right) = \frac{\tau_f'}{G}(2N_i)^{b'} + \gamma_f'(2N_i)^{c'} \tag{2}$$

where $\Delta\gamma_{\max}$ is the maximum shear strain amplitude on the critical plane, σ_y is tensile yield strength and k_2 is a correction factor. G is the shear modulus of elasticity, γ_f' is the shear fatigue ductility coefficient, and $b'$and c' are the shear fatigue strength and shear fatigue ductility exponent. The FS parameter mainly considers the maximum shear strain amplitude and uses the maximum normal stress for correction.

The SWT parameter was proposed by Smith, Watson, and Topper to improve the accuracy of predicting fatigue lifetime using only stress or strain [23]. It handles the interaction between stress and strain in fatigue lifetime prediction. The SWT parameter can be applied to both HCF and LCF conditions. In HCF, the maximum principal stress is the main influencing factor, while in LCF, strain plays the dominant role. The basic expression for SWT is given by Eq. (3):

$$SWT = \sigma_{\max}\frac{\Delta\varepsilon}{2} = \frac{\sigma_f'^2}{E}(2N_i)^{b} + \sigma_f'\varepsilon_f'(2N_i)^{b+c} \tag{3}$$

where $\sigma_{\max}$ is the maximum normal stress on the critical plane, and $\Delta\varepsilon$ is the maximum normal strain range during one cycle. σ_f' is the fatigue strength coefficient, E is Young's modulus, ε_f' is the fatigue ductility coefficient, b and c are the fatigue strength exponent and the fatigue ductility exponent. The key advantage of the SWT parameter is that it captures the combined influence of both stress and strain. The high stress accelerates crack initiation, while high strain indicates significant plastic deformation. Based on the above theory, this paper prioritizes the use of the SWT damage parameter when predicting crack initiation position, crack initiation angle and fatigue initiation lifetime. Fatigue parameters are listed in Table 3.

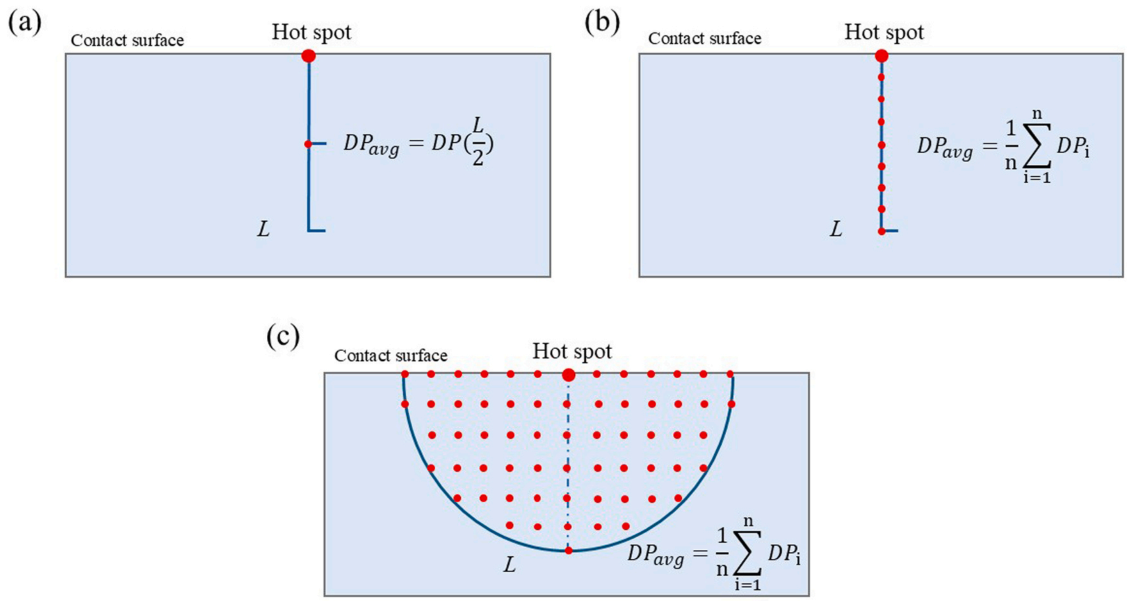

Fig. 4. Methods for averaging the damage parameter. (a) PM, (b) LM and (c) AM.

4.2. Theory of critical distances

As previously discussed, in fretting fatigue problems, the relative movement between two contact surfaces causes stress concentration on the contact surface. The TCD theory introduces a critical distance parameter, allowing consideration of the stress gradient in different stress fields. This provides a more accurate basis for averaging fatigue damage parameters and obtaining reliable fatigue life predictions. In fatigue lifetime prediction, directly using the maximum damage parameter can lead to an overly conservative estimation of lifetime. Therefore, it is necessary to average the damage parameter to introduce a specific length as a critical distance around the hotspot area. There are three common methods for averaging the damage parameter: namely Point Method (PM), Line Method (LM), and Area Method (AM) [24]. Critical distance L determines the depth from the surface. PM involves taking the damage parameter at $L/2$ as the averaged damage parameter (DP_{avg}) to estimate fatigue lifetime, as shown in Fig. 4(a). LM is averaging the damage parameters of all nodes along the length of the critical distance and using this average as the averaged damage parameter, as shown in Fig. 4(b). For AM, a semicircle is drawn with the critical distance using the radius and the contact surface as the base. The damage parameters of all nodes within this semicircular region are averaged to obtain the averaged damage parameter, as shown in Fig. 4(c).

There are also two methods for calculating the critical distance, namely fixed-TCD and variable-TCD. For fixed-TCD, the critical distance is considered as a fixed characteristic of the material. For the same material, the critical distance remains a fixed value with variations in loading conditions or the geometry of the material [25]. This constant is usually determined through fatigue testing, and its calculation formula is as shown in Eq. (4):

$$L = \frac{1}{\pi}\left(\frac{\Delta K_{th}}{\Delta \sigma_0}\right)^2 \quad (4)$$

where ΔK_{th} is the range of the threshold stress intensity factor and $\Delta\sigma_0$ is the plain fatigue limit under the same load ratio. The fixed-TCD method performs particularly well in low stress gradient problem, but it does not perform well in fatigue tests with large stress gradients. Therefore, some researchers believe that the critical distance varies with different fatigue lifetimes. Susmel and Taylor [26] proposed the variable-TCD method, as shown in Eq. (5):

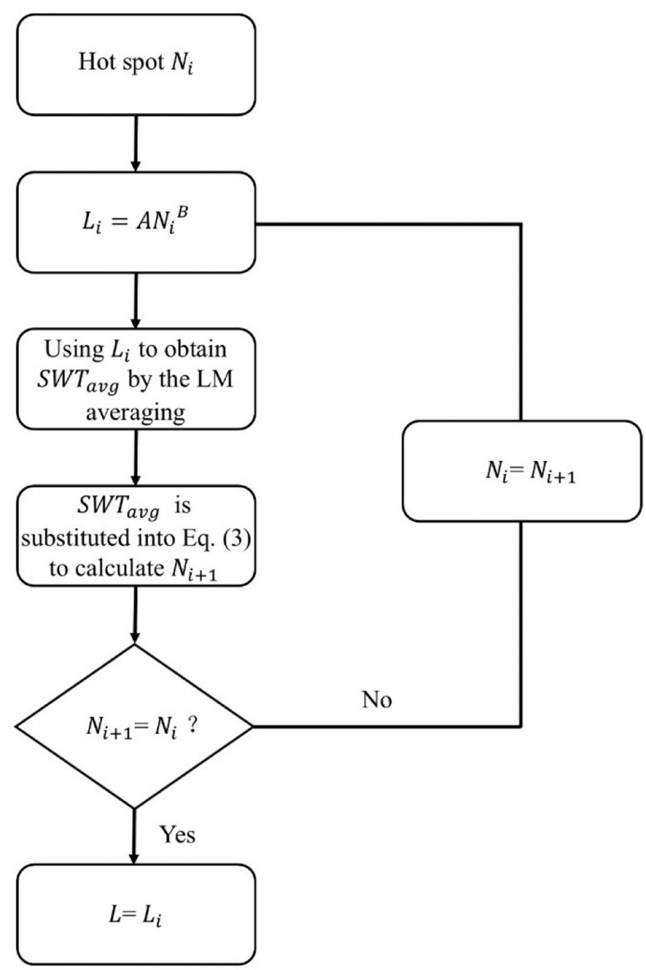

Fig. 5. Flowchart for determining the critical distance using variable-TCD.

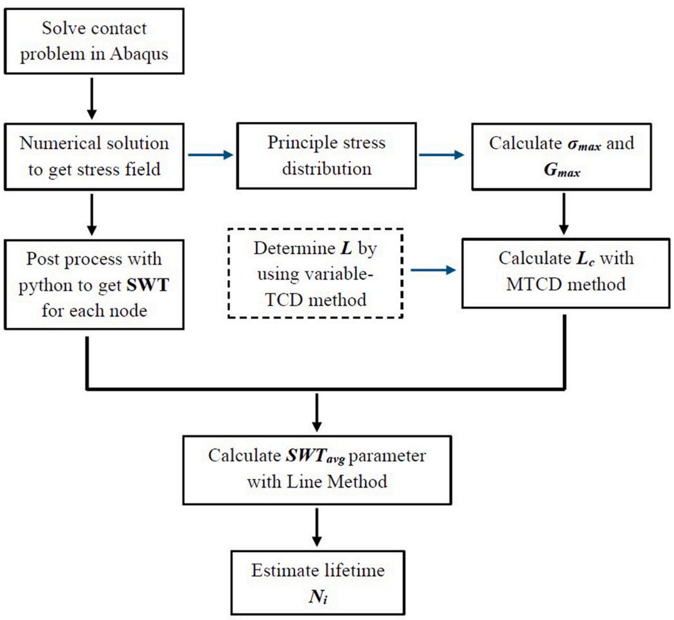

Fig. 6. Flowchart for the whole process of MTCD method.

$$L = AN_i^{\,B} \tag{5}$$

where A and B are material parameters that can be determined by combining static critical distance L (N_i=1) and high cycle critical distance L (N_i=10^7). The high cycle critical distance can be obtained by Eq. (4). The static critical distance can be calculated by Eq. (6) [27] as:

$$L = \frac{1}{\pi}\left(\frac{K_{IC}}{\sigma_{ref}}\right)^2 \tag{6}$$

where K_{IC} and σ_{ref} are material constants, i.e. mean plane strain material toughness and reference material strength, respectively. For the Ti6Al4V material, $K_{IC} = 91.45\text{MPa}\sqrt{\text{m}}$, $\sigma_{ref} = 896.07$ MPa, $\Delta K_{th} = 3.9$ MPa$\sqrt{\text{m}}$, $\Delta\sigma_0\left[10^7\right] = 538$ MPa [28], Substituting K_{IC}, σ_{ref}, ΔK_{th} and $\Delta\sigma_0\left[10^7\right]$ into Eqs. (4) and (6), the values of N_i and L are obtained. Then, by substituting the resulting N_i and L into Eq. (5), the critical distance calculation formula for Ti6Al4V can be derived, as shown in Eq. (7):

$$L = 3.317N_i^{\,-0.329} \tag{7}$$

The implementation of this method also requires following the flowchart shown in Fig. 5 to achieve convergence and determine the final critical distance. Firstly, the initial fatigue lifetime associated with the hotspot is determined by utilizing the maximum damage parameter. This initial lifetime N_i is then used as an input and substituted into Eq. (7) to obtain the critical distance L_i. Then, using the L_i to obtain SWT_{avg} by the LM averaging. Next, SWT_{avg} is substituted into Eq. (3) to calculate N_{i+1}. If $N_{i+1}$is not equal to N_i , the process moves to the next iteration. If they are equal, the loop ends and the current critical distance value is output. The above steps represent the complete process of the variable-TCD method. Under various loading conditions, the critical distance determined by the variable-TCD method demonstrates greater reliability in predicting fretting fatigue lifetime.

4.3. MTCD method

The previous discussion has established that the TCD method can effectively mitigate the impact of stress concentration on fatigue lifetime predictions. Therefore, an appropriate critical distance plays a crucial role in the validity of the predicted results. Different loading conditions can lead to various stress distributions and stress gradients, so using the fixed-TCD is evidently incorrect. Although the variable-TCD can provide different critical distances based on varying loads, it still fails to perform well in fatigue lifetime predictions for the dovetail joints.

Stress gradient refers to the rate of change of stress with respect to position, and is used to characterize the variation of the stress field in area of stress concentration. Its mathematical expression is the derivative of stress with respect to distance. In finite element analysis, the stress gradient at each node can be calculated using the numerical difference method, as shown in Eq. (8) [18]:

$$G = \frac{d_\sigma}{d_y} \approx \frac{\sigma_{i+1} - \sigma_i}{y_{i+1} - y_i} \tag{8}$$

where G is the stress gradient, σ is the principal stress, and y is the depth. In this equation, σ_{i+1} and σ_i represent the stress values at neighbouring nodes $i + 1$ and i, while $y_{i+1} - y_i$ is the distance between the two nodes. The stress gradient is used to describe the rate of change of stress, while the maximum principal stress serves as a reference for extreme stress. The two parameters complement each other, offering more reliable fatigue lifetime predictions under more complex stress conditions. For the dovetail joint, the stress distribution in the high stress concentration area is more complex. The combination of stress gradient and maximum principal stress provides a more comprehensive description of the stress distribution. Therefore, this paper introduces a MTCD method based on

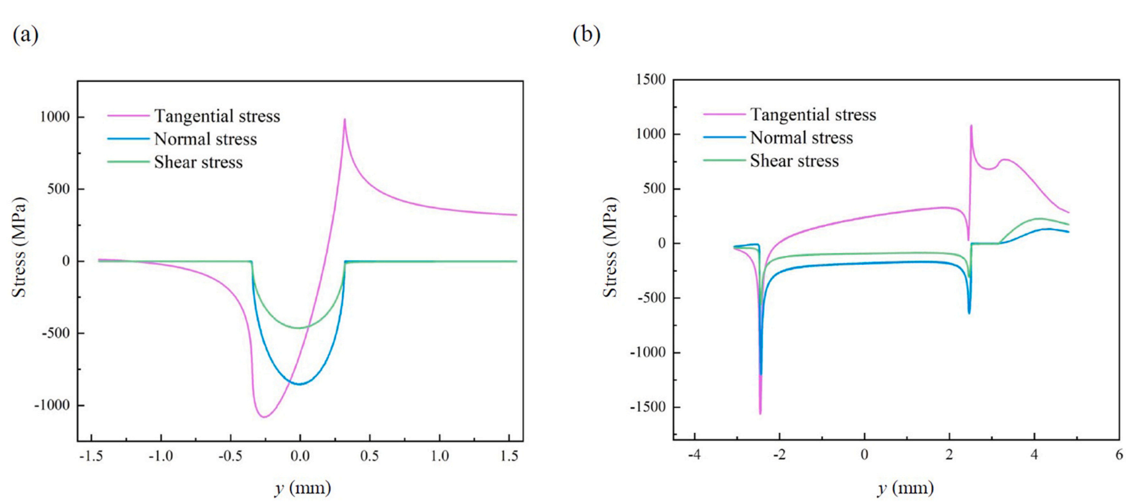

Fig. 7. Stress distribution along contact surface of two different dovetail joints under maximum load: (a) WP-T11 of dovetail joint with pads and (b) T-T3 of traditional dovetail joint.

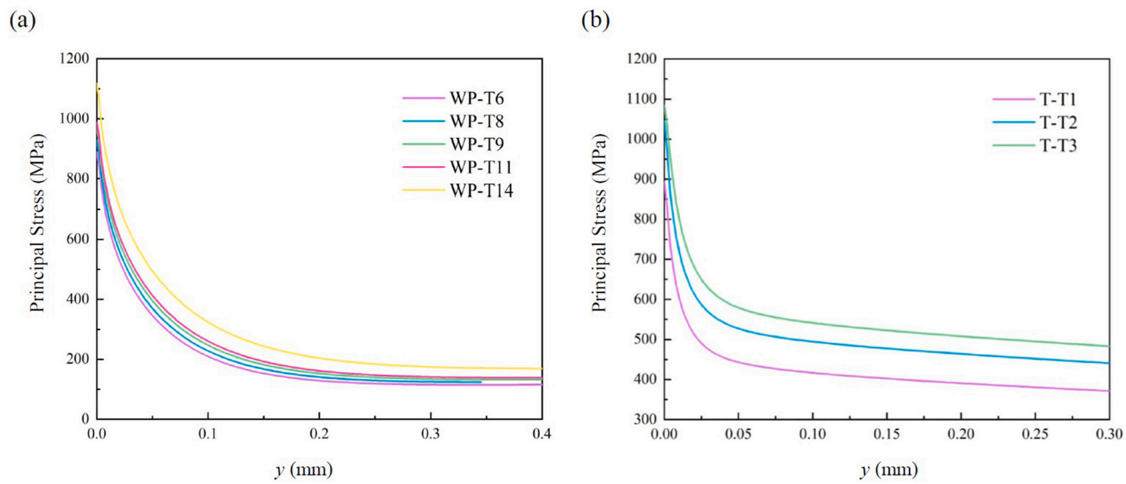

Fig. 8. Principal stress distribution along depth of the two different dovetail joints under maximum load: (a) dovetail joint with pads and (b) traditional dovetail joint.

the variable-TCD method, combining the effects of stress gradients and maximum principal stress, as shown in Eq. (9):

$$L_C = A\sqrt{\frac{\sigma_{\max}}{G_{\max}} \times L} \tag{9}$$

where A is a calibration value, $\sigma_{\max}$ is maximum principal stress, G_{max} is maximum stress gradient, and L is obtained from the variable-TCD.

To accurately estimate the crack initiation lifetime and provide a detailed and comprehensive overview of the process, a flowchart (Fig. 6) has been added to illustrate the steps from model construction to the final estimation using the MTCD method.

5. Results and discussion

5.1. Stress analysis

5.1.1. Contact stress analysis

To better analyse the stress distribution on the contact surface, Fig. 7 shows the stress distribution of two different dovetail models under maximum load. The results reveal a significant stress concentration phenomenon. Fig. 7(a) is for the dovetail joints with pads, where the purple curve represents the tangential stress. It is noticeable that there are two peaks in this curve. Along the contact surface, the tangential stress first reaches a negative maximum value on the negative side of the x-axis and then sharply rises in the opposite direction, reaching a maximum value of 986 MPa on the positive side of the x-axis. This occurs because the friction force generated by relative movement is the strongest at the edges of the contact area. Therefore, to resist this friction force, the tangential stress reaches its peak. The high tangential stress is a significant contributor to the initiation of fatigue cracks. The normal stress displays an inverted bell shape, having a peak value of −856 MPa around the centre of the contact area ($x = 0$). The shear stress has a similar profile to the normal stress, but its curve is flatter, with a smaller peak value of 464 MPa. These curves also indicate that the length of the contact area length is 0.68 mm for the dovetail joints with pads. For traditional dovetail joints, the tangential stress reaches peaks and valleys at the edges of the contact area due to the frictional force resisting the relative motion, having a peak value of 1083 MPa, as shown in Fig. 7(b). Meanwhile, the normal stress and shear stress also exhibit rapid transitions at the edges of the contact area, forming a saddle-shape profile. The figure indicates that the length of the contact area for this model is approximately 5 mm. It should be noted that although the peak stresses in both dovetail joints exceed the yield strength, the stress drops rapidly to the elastic range within 10 μm from the contact edge. Due to the obvious stress concentration/singularity at the contact interface, TCD is applied to account for this effect in the fatigue lifetime prediction, as shown in Fig. 4. The average stress obtained using TCD is significantly lower than the yield strength.

Table 4
The maximum stress gradients for the two dovetail joints under different loading conditions.

Model type	Test No.	Applied Stress (MPa)	G_{max} (MPa/mm)
Dovetail joint with pads	WP-T5	80	35164
	WP-T6	84	35544
	WP-T8	90	36008
	WP-T9	96	38366
	WP-T11	100	36585
	WP-T13	110	38002
	WP-T14	120	41045
	WP-T15	130	40405
Traditional dovetail joint	T-T1	175	47554
	T-T2	208	52819
	T-T3	228	40268

The stress distribution in the cylinder-to-flat model is relatively symmetric, mainly due to the curved geometry of the cylindrical surface, which facilitates a more uniform load distribution and reduces the stress gradient on the contact surface. In contrast, the flat-to-flat model exhibits asymmetric stress distribution due to localized stress concentrations at the contact edges, resulting in a higher stress gradient in these regions.

5.1.2. Stress gradient analysis

In fatigue analysis, due to stress concentration, a high-stress gradient tends to form on the surface of the material, leading to the occurrence of fatigue damage. Therefore, stress gradient is a critical factor influencing crack initiation and propagation. Fig. 8 represents the stress distribution curves from the surface to the core of the material under maximum load for the two different models. The vertical axis shows the principal stress, while the horizontal axis represents the depth. As the depth increases, the principal stress gradually decreases and eventually stabilizes. Fig. 8(a) shows the results of the dovetail joint with pads model. Comparing different test conditions, it is evident that different loads lead to different stress distributions, i.e. the greater the load, the higher the maximum principal stress, and the higher the stabilized value. Additionally, the rate of stress reduction (the stress gradient) varies with different loads. Similarly, the stress distribution differs across models. Fig. 8(b) shows the stress distribution of the traditional dovetail joint model, but it

Table 5
The prediction of crack initiation position for the two different dovetail joints.

Model type	Test No.	Applied Stress (MPa)	a	x/a
Dovetail joint with pads	WP-T3	75	0.290	0.993
	WP-T5	80	0.298	0.993
	WP-T6	84	0.307	0.987
	WP-T7	85	0.309	0.994
	WP-T8	90	0.318	0.994
	WP-T9	96	0.328	0.994
	WP-T11	100	0.334	0.994
	WP-T12	104	0.341	0.994
	WP-T13	110	0.351	0.994
	WP-T14	120	0.366	0.989
	WP-T15	130	0.381	0.995
Traditional dovetail joint	T-T1	175	2.504	0.999
	T-T2	208	2.501	1.000
	T-T3	228	2.503	0.999

follows the same trend as the dovetail joint with pads model. That is, as the depth increases, the principal stress decreases and eventually stabilizes, with varying stress gradients under different test conditions.

To better characterize the rate of stress variation under different loading conditions, the maximum stress gradient, G_{max}, is used in this paper. The calculated maximum stress gradients for different models under different load conditions are listed in Table 4. By comparing the five tests of the dovetail joint with pads model, it is found that although WP-T11 has a greater load, its stress gradient is smaller than that of WP-T9, which has a lower load. This conclusion also applies to the traditional dovetail joint model. T-T3 has the largest load, but its stress gradient is the smallest, while T-T2 has the largest stress gradient with a lower load than T-T3. Therefore, the stress gradient does not necessarily exhibit a strong correlation with the applied load. From a physical perspective, the stress distribution in dovetail joints is governed not only by external loads but also by contact geometry. Considering that both factors are essential for accurately characterizing the local stress state, they serve as the foundation for the development of our proposed MTCD method.

5.2. Crack initiation position and angle

The process in which microscopic defects gradually develop into visible cracks under external forces is called crack initiation. Numerical simulation plays a crucial role in the study of crack analysis [29–32]. This section analyses the initiation behaviour of cracks under fretting fatigue and uses the SWT parameter to predict the crack initiation position. The maximum SWT value indicates the position of the highest fatigue damage, where cracks are likely to initiate. To better represent the initiation position, the ratio x/a is used to describe the crack initiation position, where a represents the distance from the centre of the contact area to the edge of the contact area (1/2 the contact area length), and x represents the distance from the centre of the contact area to the location of the maximum SWT value. Table 5 shows that the contact length is increasing as the load increases in the dovetail joint with pads model and maintains a specific value in traditional dovetail joint. This is mainly due to differences in contact styles. As the load increases, the pressure on the contact surface also rises. For the cylinder-flat contact style, contact length is positively correlated with the contact pressure, whereas for the flat-flat contact style, contact length is fixed and does not change regardless of the contact pressure. By analysing the x/a in Table 5, it is evident that the value of x/a is almost unaffected by load for both models. The crack initiation position always remains at the contact area edge.

Fig. 9 shows the crack initiation angles for the two models. By comparing the angle between the crack and the contact surface, it is easily to observe that the dovetail joint with pads forms a certain angle (51°) with the contact surface, directed towards the trailing edge, the traditional dovetail joint is nearly perpendicular (100°) to the contact surface but its direction is towards the leading edge. To make a better comparison of the simulation results, the angles have been established in the global coordinate system. Fig. 9(a) represents the crack initiation angle of the dovetail joint with pads, which is 79°. Fig. 9(b) represents the crack initiation angle of the traditional dovetail joint, which is 45°.

When using the SWT parameter to predict crack initiation angles,

Table 6
The prediction of crack initiation angle for the two different dovetail joints.

Model type	Method	Simulation angle (°)	Experiment angle (°)	Difference (%)
Dovetail joint with pads	FP	76	79	3.7
	FS	74	79	6.3
	SWT	39	79	50.6
Traditional dovetail joint	FP	8	45	82.2
	FS	12	45	73.3
	SWT	50	45	11.1

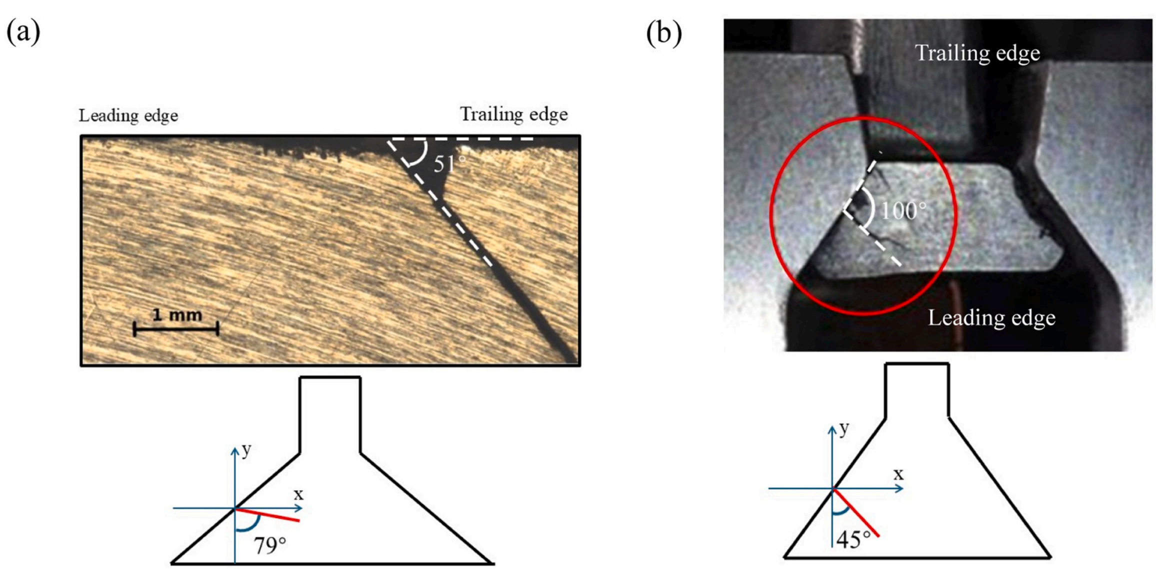

Fig. 9. Crack initiation angle of two different dovetail joints: (a) WP-T14 of dovetail joint with pads [14] and (b) T-T3 of traditional dovetail joint [19].

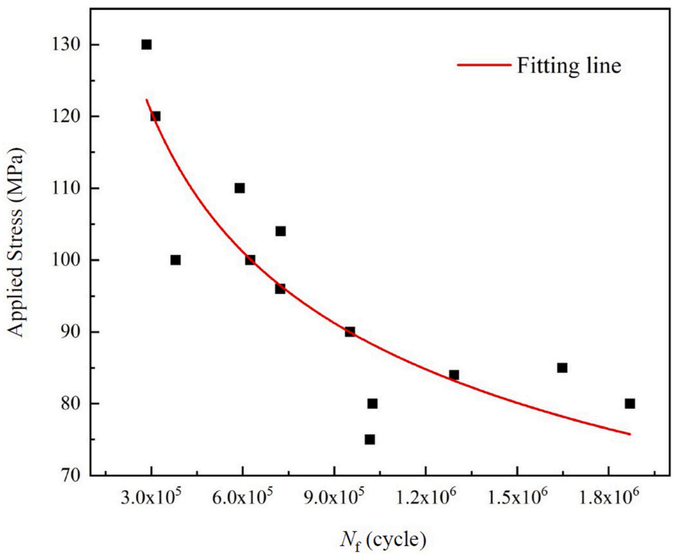

Fig. 10. Pre-processing of the dovetail joint with pads model.

different models exhibited different behaviours. Therefore, this paper utilizes three common critical plane methods (FP, FS and SWT) to predict the crack initiation angles for different models. To compare the reliability of these methods, Table 6 shows the results of different methods applied to predict crack initiation angle for the two different dovetail joints. The predictions using the FP and FS match very well with the experimental results for the dovetail joint with pads, with a difference of less than 7 %. However, the results predicted using the SWT parameter have big differences with the experimental result, with a maximum of more than 50 %. In contrast, for the traditional dovetail joint, the SWT parameter predicts the crack initiation angle with a difference of 11.1 %, while the results from the FP parameter and FS parameter show a big difference exceeding 70 % compared to the experimental results.

Cracks usually initiate along the direction of maximum shear stress (at 45°) or the direction of maximum normal stress. In the dovetail joint with pads, the crack makes 51° (approximately 45° angle) relative to the contact surface, proving that it is a crack dominated by shear stress. In the traditional dovetail joint, the crack is almost perpendicular to the contact surface, proving that the crack forms along the direction of maximum normal stress. In section 4, it has been clarified that different CP methods have different considerations. The FP parameter primarily considers the maximum shear stress amplitude, the FS parameter focuses on shear strain amplitude, while the SWT parameter considers the effects of the maximum normal stress and the strain amplitude. Based on the results, for the dovetail joint with pads, where shear stress plays a dominant role, the FP and FS parameters exhibit higher reliability in predicting the crack initiation angle. Conversely, the SWT parameter is more suitable for the traditional dovetail joint, where the maximum normal stress is the primary factor influencing crack initiation.

5.3. Prediction of fatigue initiation lifetime

5.3.1. Implementation of MTCD

The implementation of the MTCD method requires selecting a set of tests as a calibration group to obtain the parameter A in Eq. (9). Multiple influencing factors are present during the experiments process, and although strict testing methods are used to minimize testing errors, they are still inevitable. For example, in Table 1, even though the loading conditions of WP-T10 and WP-T11 are the same, their lifetimes differ by 64 %. Therefore, a pre-processing has been added in the fatigue lifetime prediction in this paper to select the calibration group and to better compare the experimental results with the simulation results.

Table 7
The critical distance for the two different dovetail joints.

Model type	Test No.	Applied Stress (MPa)	L (mm)	L_c (mm)
Dovetail joint with pads	WP-T5	80	0.034	0.042
	WP-T6	84	0.036	0.044
	WP-T8	90	0.040	0.048
	WP-T9	96	0.042	0.048
	WP-T11	100	0.046	0.052
	WP-T13	110	0.052	0.056
	WP-T14	120	0.058	0.058
	WP-T15	130	0.064	0.064
Traditional dovetail joint	T-T2	208	0.080	0.059
	T-T3	228	0.094	0.074

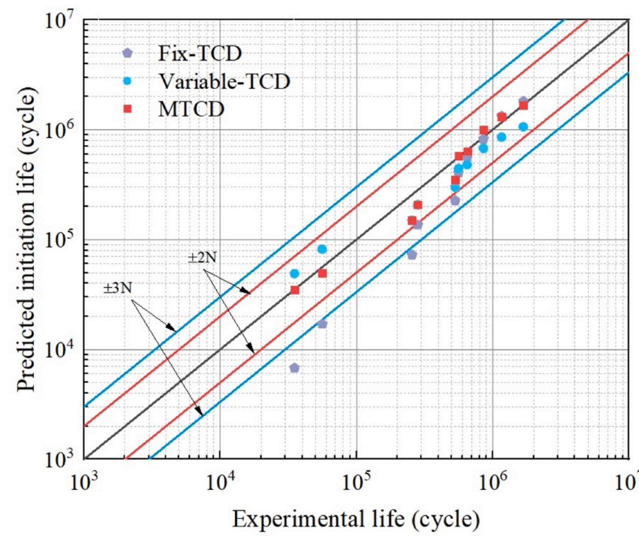

Fig. 11. Comparison of predicted crack initiation lifetimes.

In fretting fatigue, the correlation between load and fatigue lifetime follows a typical inverse exponential trend. At high stress level, fatigue lifetime decreases sharply, while at low stress level, fatigue lifetime decreases softly. This paper utilizes this rule to assess the validity of experimental results. All load and fatigue lifetime data are input to Origin software, and the relationship between load and fatigue lifetime is used to generate a fitting line. Only data points close to the fitting line are considered valid, with points falling directly on the fitting line having the highest validity and being used for calibration tests. An example of this method is shown in Fig. 10, where WP-T11 is selected as the calibration group for the dovetail joint with pads test.

Using the calibration test WP-T11 from the dovetail joint with pads model, the calibration value A can be easily obtained as 1.477, thus resulting in Eq. (10):

$$L_C = 1.477\sqrt{\frac{\sigma_{\max}}{G_{\max}}} \times L \tag{10}$$

After pre-processing the raw data, some anomalous data points are removed. The subsequent lifetime analysis is based on the following dataset: WP-T5, WP-T6, WP-T8, WP-T9, WP-T11, WP-T13, WP-T14, WP-T15 and T-T2, T-T3.

5.3.2. Results under MTCD method

Utilizing the previously described MTCD method, the data from the two models are listed in Table 7. For all models, the critical distance increases with load, regardless of the TCD method. However, for the dovetail joint with pads, the variable-TCD method is overly conservative in predicting the critical distance compared to the MTCD method.

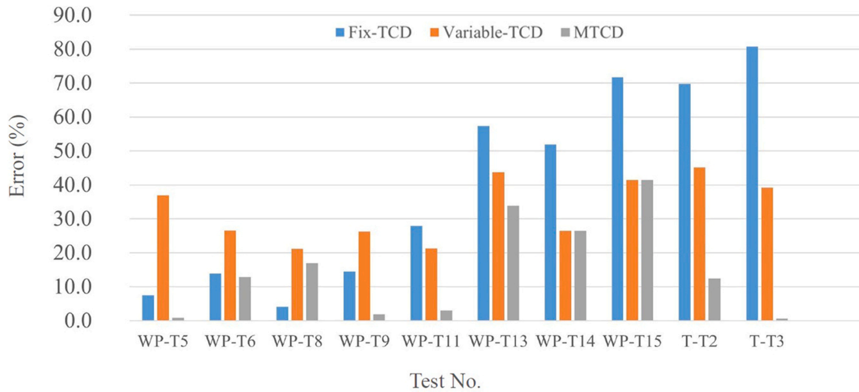

Fig. 12. Error of predicted initiation lifetimes.

Conversely, for the traditional dovetail joint, the variable-TCD method overestimates the critical distance compared to the MTCD method. Consequently, it is essential to use the MTCD method to calibrate under different models.

The previous introduction section has discussed that the initiation lifetime accounts for a large proportion of the total lifetime. In this paper, 90 % of the total lifetime is selected as the initiation lifetime. To better demonstrate the improved accuracy of the MTCD method over the fix-TCD and variable-TCD methods in predicting fretting fatigue initiation lifetime, the simulated results from this study are compared with the experimental results, as shown in Fig. 11. It is evident that all the red points are closer to the black line than the purple and blue points, with several points even directly on the black line. Both the variable-TCD and MTCD methods exhibit significantly better accuracy than the fix-TCD method, as their predicted data points mostly fall within the ± 2 N error bands, while several predictions from the fix-TCD method deviate beyond the ± 3 N range. This highlights the limitations of the fix-TCD method in capturing the fatigue initiation behaviour accurately. Furthermore, when comparing the MTCD method with the variable-TCD method, it is evident that MTCD provides even more precise predictions, with many data points aligning almost perfectly with the experimental values. In summary, the MTCD method proposed in this paper demonstrates higher reliability in predicting fretting fatigue crack initiation lifetime.

To further know the difference of predicted crack initiation lifetimes among the three methods, an error comparison is presented in Fig. 12. The error is calculated by Eq. (11), where N_e is the experimental initiation lifetime, and N_p is the predicted initiation lifetime using different methods:

$$Error = \frac{|N_e - N_p|}{N_e} \times 100\% \tag{11}$$

For most test cases, the MTCD method achieves significantly lower error percentages compared to fix-TCD and variable-TCD. In particular, WP-T5 and T-T3 show near-zero error (0.8 % and 0.6 %), demonstrating the superior accuracy of MTCD.

6. Conclusions

This paper is based on fretting fatigue tests of two dovetail joint models, analysing the stress distribution of both models, studying the crack initiation locations and angles, and predicting the fatigue initiation lifetime. Based on the numerical simulations, the following conclusions have been drawn:

1. As the load increases, the length of the contact area for the dovetail joint with pads increases, while it remains nearly unchanged for the traditional dovetail joint.
2. In both dovetail joints, the maximum principal stress shows a positive correlation with increasing load. However, the value of the stress gradient is not necessarily strongly correlated with the magnitude of the load.
3. For the dovetail joint with pads, the FP and FS parameters exhibit higher reliability in predicting the crack initiation angle. Conversely, the SWT parameter is more suitable for the traditional dovetail joint.
4. A pre-processing step has been added in the fatigue lifetime prediction to select a more accurate calibration group, allowing for better comparison of the test results with the simulation results.
5. A Modified Theory of Critical Distances (MTCD) has been proposed, integrating the effects of stress gradients and maximum principal stress, resulting in more precise predictions of fatigue initiation lifetime.

Statement of novelty

Under fretting conditions in dovetail joints, the stress-strain distribution on the contact surface becomes more complex, affecting the applicability of different criteria. This study examines the stress states across various models and evaluates the suitability of each criterion accordingly. The accuracy of crack initiation angles prediction for two dovetail joints is improved.

The maximum principal stress serves as a reference for extreme stress and the stress gradient is used to describe the rate of change of stress. The combination of stress gradient and maximum principal stress provides a more comprehensive description of the stress distribution, A Modified Theory of Critical Distances (MTCD) is introduced, integrating stress gradients and maximum principal stress, to improve fretting fatigue lifetime predictions in dovetail joints. Unlike traditional TCD methods, the modified approach accurately addresses complex stress distributions, offering more precise predictions of crack initiation.

CRediT authorship contribution statement

Wang Dagang: Writing – review & editing. **Wang Can:** Software, Investigation. **Ahmed Bilal:** Investigation. **Xiao Qiqi:** Writing – review & editing, Methodology, Investigation, Conceptualization. **Abdel Wahab Magd:** Writing – review & editing, Supervision, Investigation, Conceptualization. **Cai Zhenbing:** Writing – review & editing. **Wang Lihua:** Writing – review & editing, Supervision.

Declaration of Competing Interest

The authors declare that they have no known competing financial interests or personal relationships that could have appeared to influence the work reported in this paper.

Acknowledgment

The authors acknowledge the support of National Natural Science Foundation of China (Grant Nos. 52175205 and 51875565). This work is supported by the National Natural Science Foundation of China (Project no. 12272270) and the Shanghai Pilot Program for Basic Research.

Data availability

Data will be made available on request.

References

[1] Sunde SL, Berto F, Haugen B. Predicting fretting fatigue in engineering design. Int J Fatigue 2018;117:314–26.
[2] Shen F, Ke L-L, Zhou K. A debris layer evolution-based model for predicting both fretting wear and fretting fatigue lifetime. Int J Fatigue 2021;142:105928.
[3] Pereira K, Bordas S, Tomar S, Trobec R, Depolli M, Kosec G, Abdel Wahab M. On the Convergence of Stresses in Fretting Fatigue. Materials 2016.
[4] Wang S, Yue T, Wang D, Abdel Wahab M. Effect of wear debris on fretting fatigue crack initiation. Friction 2022;10(6):927–43.
[5] Chen X, Wang J, Lu L, Zou L, Xu T, Dong Y, Zhao H, Zeng D. Effect of interference magnitude on fretting wear and fatigue strength of scaled press-fitted railway axles. Wear 2024;546-547:205347.
[6] Venugopal Poovakaud V, Jiménez-Peña C, Talemi R, Coppieters S, Debruyne D. Assessment of fretting fatigue in high strength steel bolted connections with simplified Fe modelling techniques. Tribology Int 2020;143:106083.
[7] Sadeghi M, Abdel Wahab M, Hojjati Talemi R, Yue T. A review of FE on crack initiation in fretting fatigue. 5th Int Conf Sustain Constr Des (SCAD-2013) 2013.
[8] Szolwinski MP, Farris TN. Observation, analysis and prediction of fretting fatigue in 2024-T351 aluminum alloy. Wear 1998;221(1):24–36.
[9] Sunde SL, Haugen B, Berto F. Experimental and numerical fretting fatigue using a new test fixture. Int J Fatigue 2021;143:106011.
[10] Wang C, Wang D, Wahab MAbdel. Fretting fatigue crack initiation behaviour in heterogeneous materials under out-of-phase loading. Tribology Int 2022;171:107571.
[11] Wang C, Fan K, Zhao Q, Wahab MAbdel. Effect of shot peening parameters on fretting fatigue lifetime. Tribology Int 2024;193:109311.
[12] Hao R, Wen Z, Xin H, Lin W. Fatigue Life Prediction of Notched Details Using SWT Model and LEFM-Based Approach. Materials 2023.
[13] Kouanga CT, Jones JD, Revill I, Wormald A, Nowell D, Dwyer-Joyce RS, Araújo JA, Susmel L. On the estimation of finite lifetime under fretting fatigue loading. Int J Fatigue 2018;112:138–52.
[14] Zhu X, Chen X. Fretting fatigue life prediction of full-scale dovetail joints using the theory of critical distances with mesh control. Tribology Int 2024;199:110063.
[15] Araújo JA, Susmel L, Taylor D, Ferro JCT, Mamiya EN. On the use of the Theory of Critical Distances and the Modified Wöhler Curve Method to estimate fretting fatigue strength of cylindrical contacts. Int J Fatigue 2007;29(1):95–107.
[16] Shi L, Wei D-s, Wang Y-r, Tian A-m, Li D. An investigation of fretting fatigue in a circular arc dovetail assembly. Int J Fatigue 2016;82:226–37.
[17] Shen J, Fan H, Zhang G, Pan R, Wang J, Huang Z. Influence of the stress gradient at the notch on the critical distance and life prediction in HCF and VHCF. Int J Fatigue 2022;162:107003.
[18] Zhu X, Chen X. A modified critical distance method for estimating fretting fatigue life of dovetail joints. Fatigue Fract Eng Mater Struct 2024;47:4132–50.
[19] Hu C, Wei D, Wang Y, Shi L. Experimental and numerical study of fretting fatigue in dovetail assembly using a total life prediction model. Eng Fract Mech 2019;205:301–18.
[20] Yao S-L, Zeng X-T, Li K-S, Wang J, Wang R-Z, Wang N, Zhang C-C, Zhang X-C, Tu S-T. Fretting fatigue life improvement of nickel-based superalloy GH4169 dovetail slots by deflecting abrasive waterjet peening process. Int J Fatigue 2023;175:107832.
[21] Bhatti NA, Abdel Wahab M. A numerical investigation on critical plane orientation and initiation lifetimes in fretting fatigue under out of phase loading conditions. Tribology Int 2017;115:307–18.
[22] Díez Molina N, Vanegas Useche LV, Mesa CA, Wang C, Wang L, Wahab MAbdel. Fretting fatigue crack nucleation analysis under a variable coefficient of friction. Tribology Int 2024;194:109558.
[23] Rangel D, Erena D, Vázquez J, Araújo JA. Prediction of initiation and total life in fretting fatigue considering kinked cracks. Theor Appl Fract Mech 2022;119:103345.
[24] Wang C, Li C, Ling Y, Wahab MAbdel. Investigation on fretting fatigue crack initiation in heterogenous materials using a hybrid of multiscale homogenization and direct numerical simulation. Tribology Int 2022;169:107470.
[25] Men H, Zhou W, Huang H, Wang M, Fu X. Study of the Point Method for fretting fatigue life prediction. Int J Mech Sci 2024;275:109297.
[26] Susmel L, Taylor D. A novel formulation of the theory of critical distances to estimate lifetime of notched components in the medium-cycle fatigue regime. Fatigue Fract Eng Mater Struct 2007;30(7):567–81.
[27] Deng Q, Yin X, Wang D, Wahab MAbdel. Numerical analysis of crack propagation in fretting fatigue specimen repaired by stop hole method. Int J Fatigue 2022;156:106640.
[28] Yamashita Y, Ueda Y, Kuroki H, Shinozaki M. Fatigue life prediction of small notched Ti–6Al–4V specimens using critical distance. Eng Fract Mech 2010;77(9):1439–53.
[29] Rabczuk T, Belytschko T. Cracking particles: a simplified meshfree method for arbitrary evolving cracks. Int J Numer Methods Eng 2004;61(13):2316–43.
[30] Rabczuk T, Belytschko T. A three-dimensional large deformation meshfree method for arbitrary evolving cracks. Comput Methods Appl Mech Eng 2007;196(29):2777–99.
[31] Goswami S, Anitescu C, Chakraborty S, Rabczuk T. Transfer learning enhanced physics informed neural network for phase-field modeling of fracture. Theor Appl Fract Mech 2020;106:102447.
[32] Samaniego E, Anitescu C, Goswami S, Nguyen-Thanh VM, Guo H, Hamdia K, Zhuang X, Rabczuk T. An energy approach to the solution of partial differential equations in computational mechanics via machine learning: concepts, implementation and applications. Comput Methods Appl Mech Eng 2020;362:112790.